Mater Eng Res, 2022, 4(1): 223-235
DOI: 10.25082/MER.2022.01.004

RESEARCH ARTICLE

Degradation mechanisms of zinc-air batteries used in hearing aid

Kelly Hunt[1] **Mallory Bates**[1] **Gerard Klint Simon**[2] **Tarun Goswami**[1*]

[1] Department of Biomedical, Industrial and Human Factors Engineering, Wright State University, Dayton, OH 45435, USA
[2] Materials and Manufacturing Directorate, Air Force Research Laboratory, Wright Patterson Air Force Base, Dayton, OH 45433 USA

Correspondence to: Tarun Goswami, Department of Biomedical, Industrial and Human Factors Engineering, Wright State University, Dayton, OH 45435, USA; Email: tarun.goswami@wright.edu

Received: March 22, 2022;
Accepted: May 20, 2022;
Published: May 25, 2022.

Citation: Hunt K, Bates M, Simon GK, *et al*. Degradation mechanisms of zinc-air batteries used in hearing aid. *Mater Eng Ress*, 2022, **4**(1): 223-235. https://doi.org/10.25082/MER.2022.01.004

Abstract: Hearing aid devices are powered by the oxidation of zinc that occurs within zinc-air batteries. Zinc-air batteries have an average discharge time of 7 days. Therefore, hearing-aid devices need frequent battery replacement. In this paper, degradation mechanisms of zinc-air batteries investigated where a competition mechanism between zinc passivation and dendritic formation dictates the battery life. This research included exposure time from none to 9 days and to document dendritic growth with time. Scanning electron microscope images were taken to quantify the damage growth as well energy dispersive X-ray tests were conducted to comment on the composition changes. The results confirmed an increase in oxygen in exposed batteries from unexposed. These results matched findings from past literature. Exposure time was investigated to optimize battery lifespan. In conclusion, life of zinc-air batteries depends on the competition mechanism of zinc passivation and dendritic formation caused by oxidation and our investigation shows that this occurs within the first 7 days.

Keywords: hearing aid, zinc-air batteries, oxidation, dendrites, exposure time, SEM

1 Introduction

Zinc-air batteries are the gold standard power supply for hearing aid devices (HAD). These batteries are available in different sizes correlating to their respective capacity that ranges from 91 to 620 mAh. Discharge begins with the removal of a thin film covering the battery surface and preforms uniformly, reaching zero capacity after 7 days on average. These batteries present limitations related zinc passivation, dendritic formation, and electrolyte dehydration. Extensive research has been done on these failure mechanisms and how to correct the weaknesses of the battery supply.

The cathode and anode of the battery are constructed different than a traditional alkaline battery. The cathode is not physically present in the cell but is the presence of oxygen in the atmosphere. This is referred to as an air cathode. The air enters the battery cell and interacts with the electrolyte to transfer electrons to the anode (Equation (1)). Including this aspect in the design reduces the overall size of the battery but can be the reason for the diminished life span. The anode is composed of zinc fibers. These fibers react with hydroxyl molecules to create zinc hydroxide, which dissociates back to zinc oxide, water, and hydroxyl molecules (Equation (2) and (3)). Between the anode and cathode is the electrolyte. Traditionally, this electrolyte is a potassium hydroxide material. The electrolyte transfers electrons from the cathode to the anode and creates the electrical current that powers the device. Below, basic cathode and anode reactions are presented in Equation (1), (2) and (3), respectively. The reaction at the anode occurs in two separate steps as zinc reacts with the electrolyte.

(1) Cathode (air electrode) reaction:

$$^1/_2O_2 + H_2O + 2e^- \rightarrow 2OH^- \quad (1)$$

(2) Anode (Zinc electrode) reaction:

$$Zn + 4OH^- \rightarrow Zn(OH)_4{}^{2-} + 2e^- \quad (2)$$

$$Zn(OH)_4{}^{2-} \rightarrow ZnO + H_2O + 2OH^- \quad (3)$$

To address the limitations of the battery cell, several researchers have investigated the use of alternative electrolytes, anode coatings, and pulsed depositions. Others have a lot forgone the use of zinc-air battery cells and proposed the use of lithium batteries in HAD.

In this paper, the failure mechanisms of zinc air batteries will first be discussed as well as how other workers have attempted to correct these limitations. Then, this research will be discussed,

in which the physical decay of the anode and electrolyte during air exposure is observed with scanning electron microscopy. These images and data were compared to software generated zinc air battery reactions (Equation (1). (2) and (3)). Using this data, a mathematical model for zinc air battery degradation was formulated.

2 Failure mechanisms and corrections

2.1 Zinc passivation

When the reaction occurs between the electrolyte and anode, zinc is oxidized, producing a solid zinc oxide layer on the anode. This process is called zinc passivation. When ZnO precipitates on the anode, zinc dissolution is halted and capacity is reduced [1]. If enough precipitate is accumulated, the battery cell will reach failure. As the current density and electrolytic concentration increases, the rate at which zinc passivation occurs is expedited [2]. This process is widely studied because of high occurrence in all zinc air batteries and because the physical layer of zinc precipitate is visible with only optical microscopy [2].

In some of the research, it has been noted that as zinc-oxide accumulates, only once it reaches a critical concentration will it cause passivation the battery cell and prevent further electrochemical reactions [2]. This critical concentration causes a color change from light yellow to brown, which is also easily seen under microscopy.

Zinc passivation has been explained using three different models, the "dissolution-precipitation" model, the "adsorption" model, and the "nucleation and growth" model, although all explain the same end result of reduced capacity [2]. Using data from experiments, Liu et al. formulated an equation to predict the time to passivation, represented by variable k (Equation (4)) [3].

$$k = \left(\frac{\varepsilon^{(1+\tau)} D_b C_b}{\bar{V}_{\text{Znoy}} \cdot \left(\frac{(4-2y)}{n\boldsymbol{F}} + \frac{t_0}{z\boldsymbol{F}} \right)} \right)^{\frac{1}{2}} \tag{4}$$

With this equation, the time from first discharge until the anodic reaction will cease can be estimated. Using Equation (4) and other experimental data, several researchers investigated zinc passivation correction by altering electrolyte concentration [4], coating the anode zinc-particles in silica [5], changing the pH of the electrolyte [4], and using a gelled electrolyte rather than aqueous [6]. Additionally, Kim et al. investigated the process of limiting zincate ions released into aqueous solution to secure the concentration to be less than that of the solubility limit in solution [7].

2.2 Dendritic formation

Dendrites are small branches that can form on the zinc fibers of the anode. These branches create a change in shape to the particles and to the anode itself. They are caused by the ionic transfer, migration, and convection during diffusion [8]. With a confirmation change, the reaction between the electrolyte and anode is altered, and thus the capacity of the battery is reduced. Dendrites introduce potential risk of short circuiting the cell [9]. If short circuited, the battery will immediately stop all power output to the associated device and can cause harm to the user [10]. They can also increase the occurrence of passivation, which limits the overall capacity of the battery cell as mentioned previously [10].

This limitation has been investigated by institutions and potential corrections have been proposed. At the Clausthal University of Technology, researchers have experimented with varying current densities in addition to flowing electrolyte to reduce overall dendritic growth [11]. They found that a lower current density coupled with the flowing electrolyte would reduce the overall dendritic formation and extend the battery life [11].

Many others approach this limitation by introducing additives to the battery cell. Case Western University, Pusan National University, and Zhejiang University investigated the addition of polyethylene glycol, tin, and bismuth ion and tetrabutylammonium bromide, respectively, to electrolytes and anodes to limit dendritic formation and growth [12–14]. All studies exhibited success with the electrolyte additives and an extended life cycle due to limitation of dendritic growth at the anode as well as a decrease of zinc passivation.

3 Experimental details

3.1 Materials

Two packages of eight, size 13 Energizer zinc air batteries were purchased. During the process, the packages were left in a well-ventilated fume hood. Other materials included a

diamond cutter, scanning electron microscope (SEM), latex free balloons, and argon-filled glove box. The SEM used was a ThermoFisher Scientific Quanta FEG 650 edition.

3.2 Experiment I procedure

3.2.1 Day 1

On day 1, one battery was transported to Wright Patterson Air Force Base in Dayton, Ohio. This battery was left sealed in with the original covering during transport. Upon arrival at the research laboratory, the battery was sliced in half vertically with a diamond cutter without coolant. Both halves of the battery were immediately placed into sealed balloon. This ensured that very little reaction with oxygen would occur prior to imaging. The balloon was transferred to the argon glove box with 1ppm O_2 and 1ppm H_2O. The balloon was opened in the glove box, one half of the battery was removed, and an SEM imaging plate made of copper was created in the glove box with a portion of interior ingredients of the battery. Both halves were placed back into the balloon, sealed, and left in the glove box. The SEM plate was removed from the glove box at 16:04 on day 1 and transferred to the SEM. At 16:09, the sample plate was inserted in the SEM and pressurizing began. The final SEM state included a chamber pressure of 4.68 E -5 Torr, gun pressure of 9.06 E -10 Torr, and emission current of 142 μA. The microscope was focused on the sample at a distance of 10 mm. For the next 30 minutes, images and Energy Dispersive X-Ray Spectroscopy (EDS) data was collected. The sample was removed from the SEM at 17:10, placed into the SEM plate carrying case, and left to sit at room temperature for 23 hours.

3.2.2 Days 2,3,4,7

Using the same SEM plate, images and EDS data were collected for the next seven days at approximately 16:00 each day. The chamber pressure, gun pressure, and emission current remained constant during all data collections, and the stage was set to 10 mm for all photo acquisition. Data was not collected on days 5 and 6 due to inability to access the SEM per institution regulations.

3.2.3 Day 9

On day 9, the sample from the glove box was removed at 16:06. The sample was left in the balloon and transported to the SEM location. Here, the balloon was opened, sample extracted, and SEM plate created on a copper mounting plate. The plate was then inserted into the SEM at 16:16 and imaging began with the same imaging conditions as the previous days. Both images and EDS data were collected for this sample.

3.3 Experiment II procedures

On day 1 of this experiment, each of the batteries were opened for a period of time and then reclosed until testing with a control battery that was not reclosed. The time intervals were 1 minute, 30 minutes, 1 hour, 2 hours, 3 hours, and control. The batteries were reclosed by placing the flap back into place, that is removed originally.

The batteries were imaged 4 days later, based on the results from Experiment 1. The batteries were sliced vertically with a diamond cutter. The batteries were then placed in an SEM machine with the same conditions as Experiment 1 and images were taken.

3.4 Image analysis

Images collected with the SEM were analyzed with ImageJ software. Image processing was used by putting a threshold on the images. A scale was set based upon given measurements. Certain elements of the images were highlighted, which were put in an interactive 3-D plot. The plot shows the depth of these highlighted elements. A varying magnification was given each day based upon the presence of oxidation. Day 1, 7, and unexposed were uploaded at the lowest magnification.

4 Results

4.1 Experiment I results

The images and corresponding EDS collections are displayed according to the day obtained and sample type (Figure 1 to 13). The image analysis with 3-D interactive plots (Figure 14 to 16).

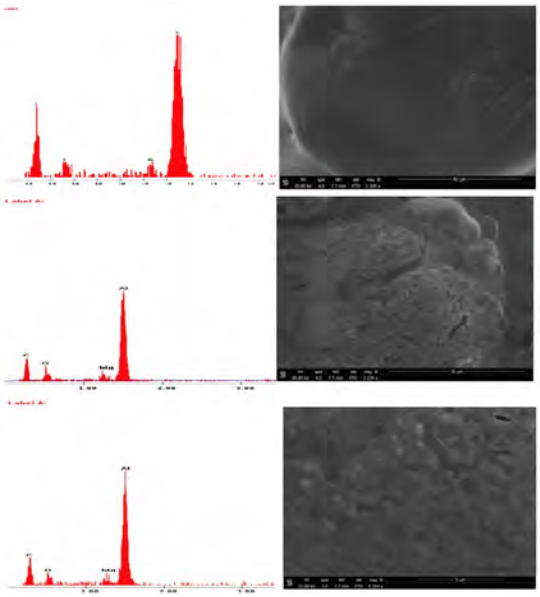

Figure 1 Day One exposed battery SEM and EDS data

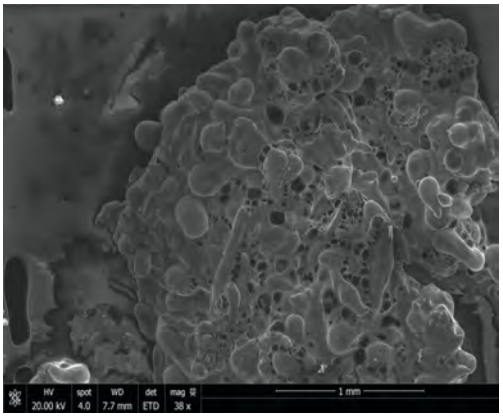

Figure 2 Day one exposed Battery SEM overview

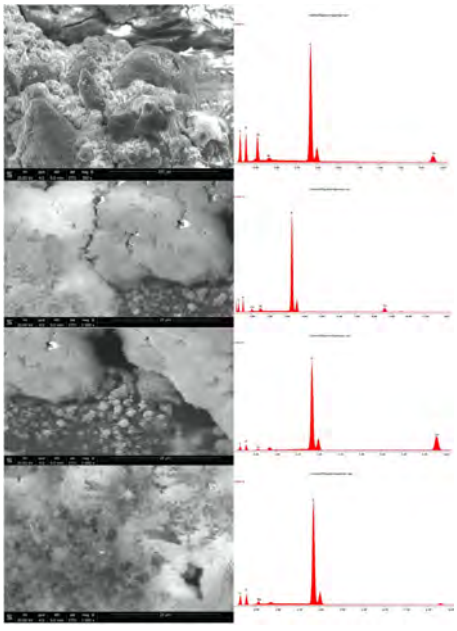

Figure 3 Day two exposed battery SEM and EDS data

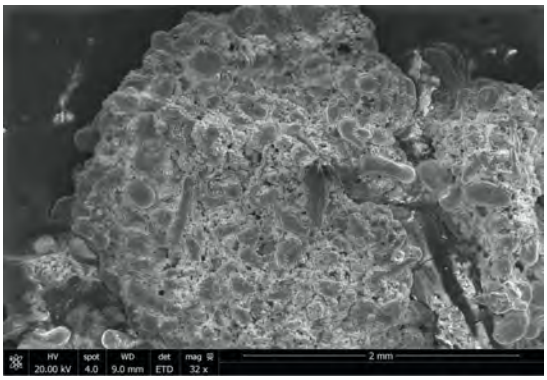

Figure 4 Day two exposed battery SEM overview

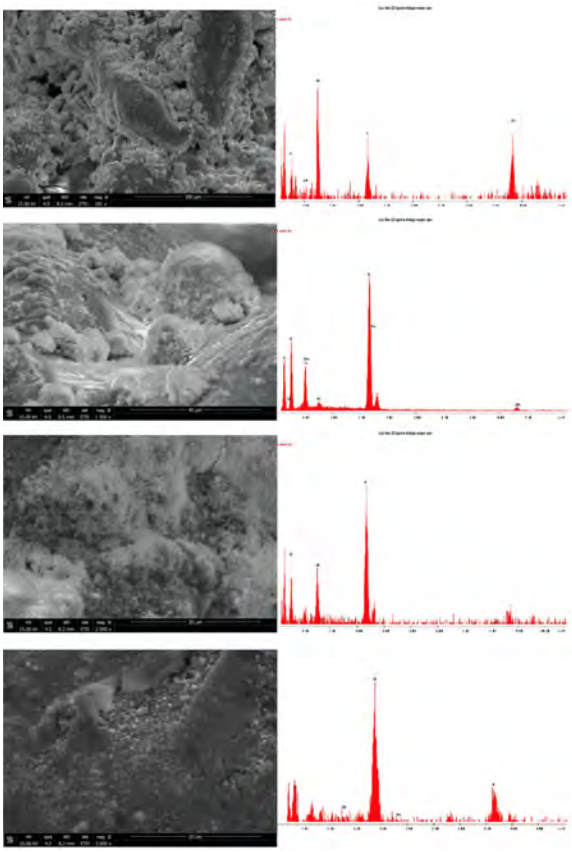

Figure 5 Day three exposed battery SEM and EDS data

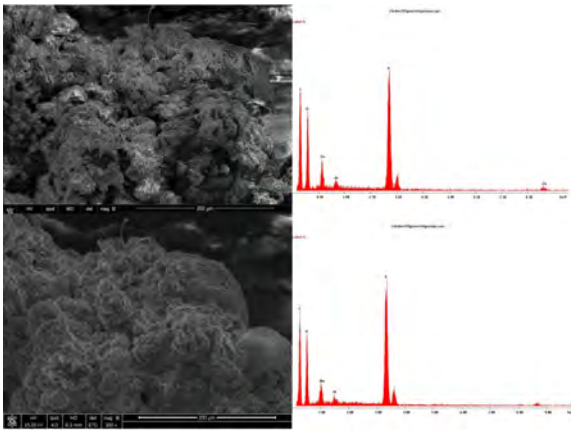

Figure 6 Day four exposed battery SEM and EDS data

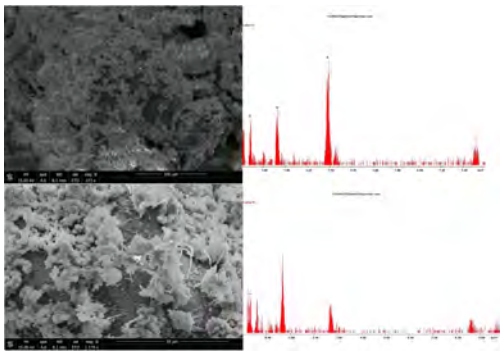

Figure 7 Day four exposed battery SEM and EDS data presenting dendritic structures

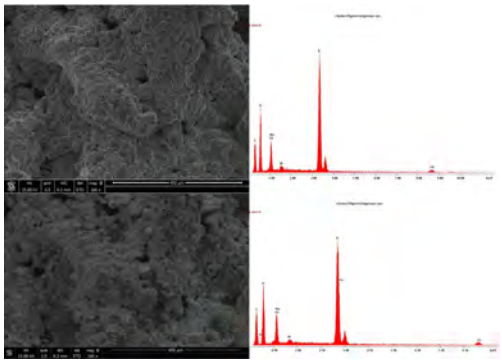

Figure 8 Day seven exposed battery SEM and EDS data

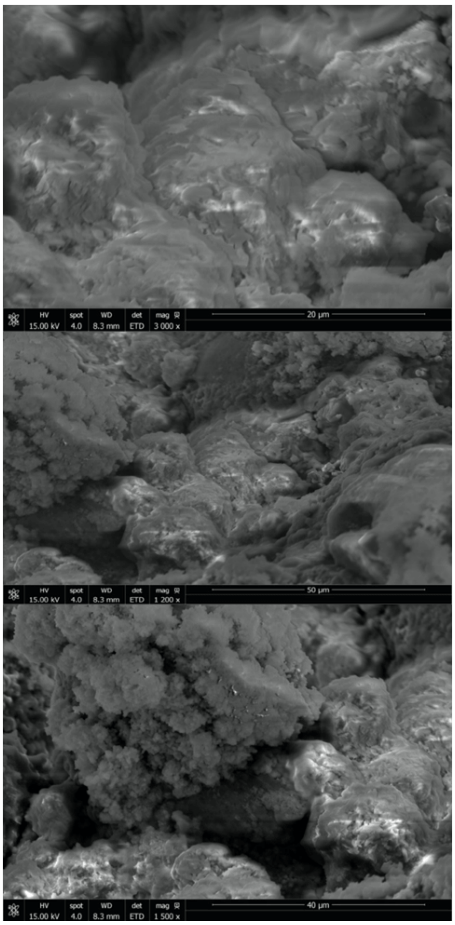

Figure 9 Additional day four exposed battery SEM and EDS data

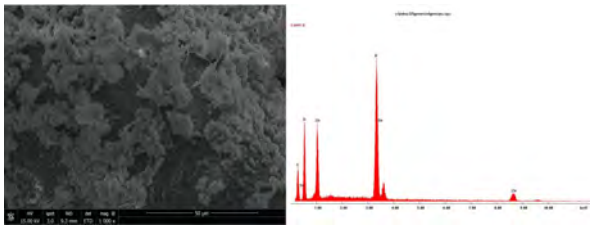

Figure 10 Day seven exposed battery SEM and EDS data presenting dendritic structures

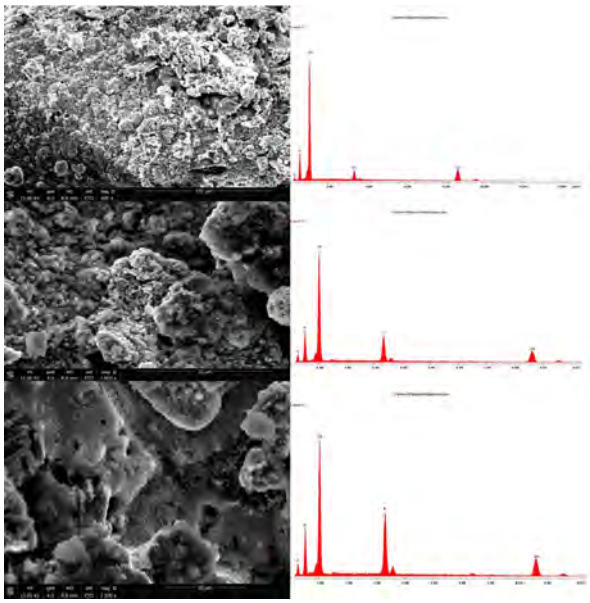

Figure 11 Day nine unexposed battery SEM and EDS data

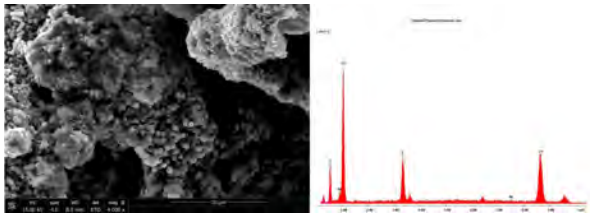

Figure 12 Additional day nine unexposed battery SEM and EDS data

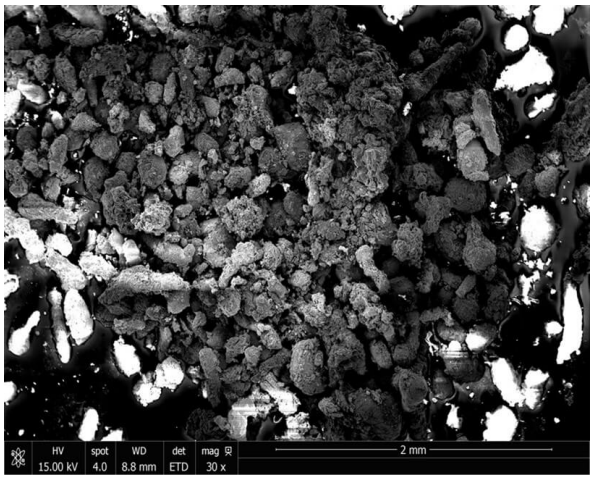

Figure 13 Day nine unexposed battery SEM image

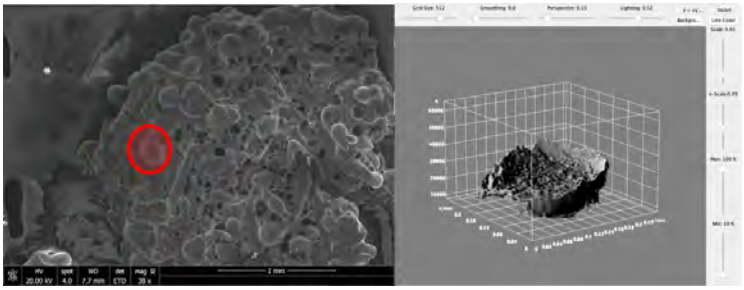

Figure 14 Day 1 exposed highlighted section and 3-D interactive plot

Figure 15 Day 7 exposed highlighted section and 3-D interactive plot

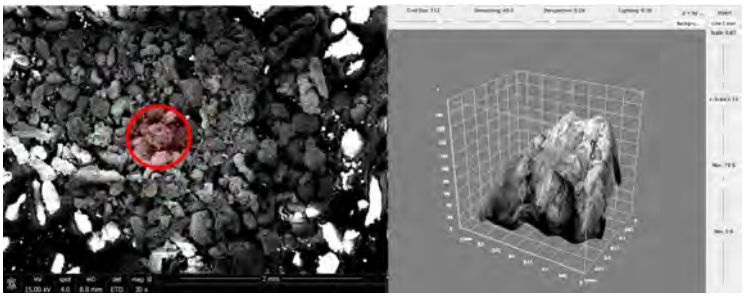

Figure 16 Unexposed highlighted section and 3-D interactive plot

4.2 Experiment II results

The images are displayed according to time interval (Figure 17 to 22).

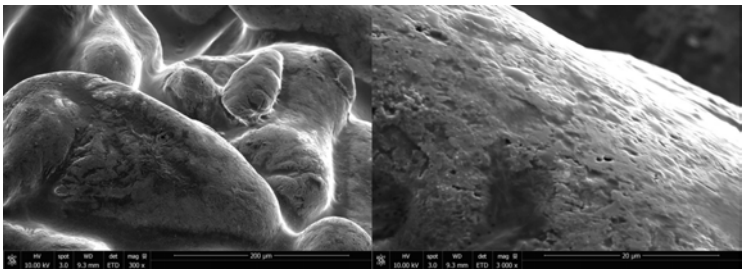

Figure 17 One minute exposure time SEM images

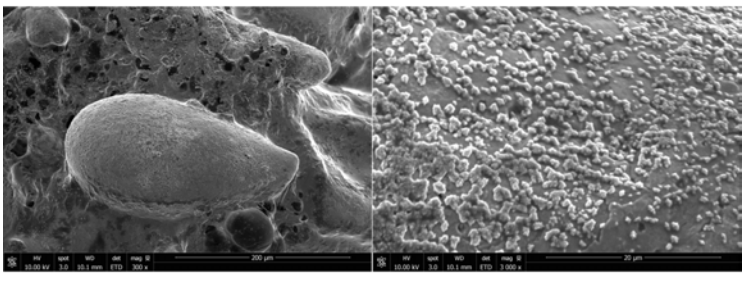

Figure 18 Thirty minutes exposure time SEM images

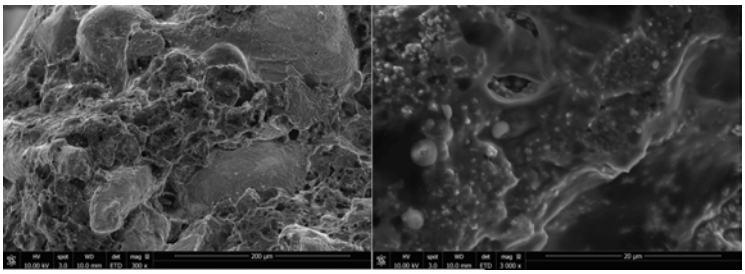

Figure 19 One hour exposure time SEM images

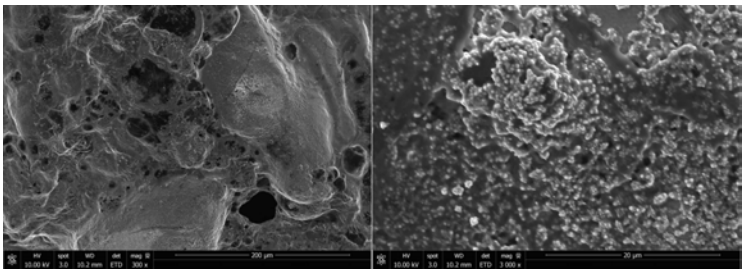

Figure 20 Two hour exposure time SEM images

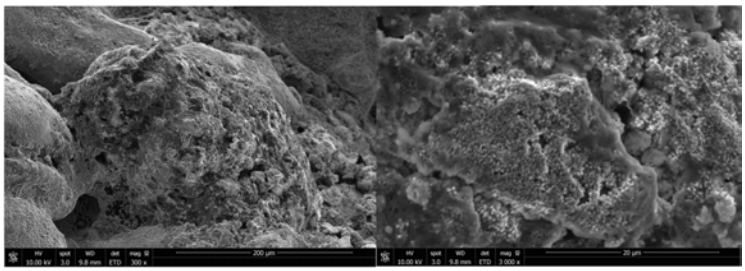

Figure 21 Three hour exposure time SEM images

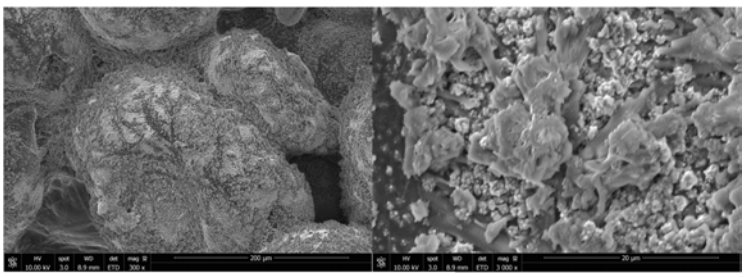

Figure 22 Four days exposure time SEM images (control)

5 Discussion

Utilizing both SEM micrographs and EDS analysis, as well as the literature previously published, our findings are consistent with that of others discussed below.

The difference between the unexposed and exposed batteries after full exposure was analyzed first. The percent compositions gathered via the EDS process as well as the accompanying literature and prior findings, can be utilized to build further conclusions and connections between exposed and unexposed batteries. The compositions considered were carbon, oxygen, potassium, and zinc, which are the main components in the battery and play important roles in the reaction process. The two batteries compared were the day 7 exposed battery and day 9 unexposed battery (Figure 23). These two micrographs represent the end result in each exposure environment. In Table 1 and Figure 24, the percentage of carbon, oxygen, potassium, and zinc of both the day 7 exposed battery and day 9 unexposed battery are displayed. Of this data, the value of highest concern is the oxygen amount variation in the two batteries. While the unexposed battery (*battery B*, Figure 23) does have some oxygen, the exposed battery (*battery A*, Figure 23) 257% more oxygen present. Even though the unexposed battery has not been subjected to

the atmosphere and oxygen, there is still oxygen present in the electrolyte compound, KOH. Regardless of this small addition of oxygen in both batteries, the steep increase of oxygen in the exposed battery indicates that the process of zinc oxidation has occurred.

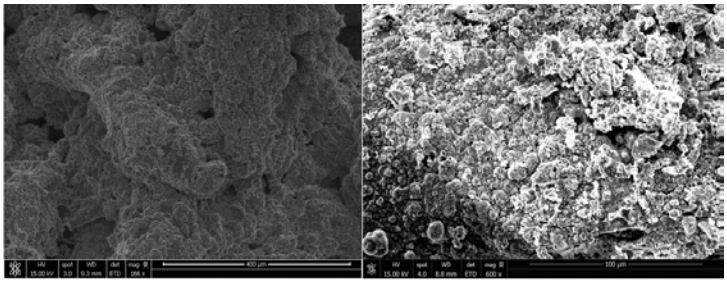

Figure 23 (A) Day 7 SEM image of the exposed battery sample at 166x magnification; (B) Day 9 SEM image of the unexposed battery sample at 600x magnification.

Table 1 Percentages of carbon, oxygen, potassium, and zinc present in day 7 exposed battery and day 9 unexposed battery

Battery Type	Element Percentage			
	C	O	K	Zn
Day 7, exposed	13.200	27.725	40.275	20.565
Day 9, unexposed	5.675	10.803	9.610	73.913

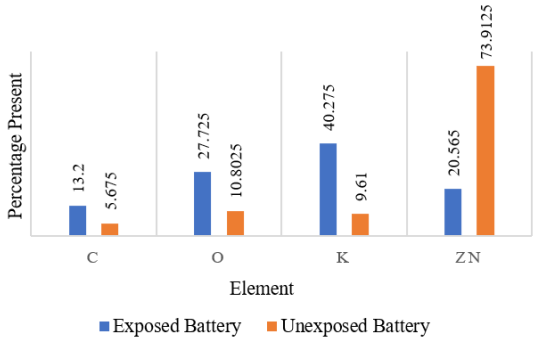

Figure 24 Elemental percentage composition of exposed battery verses unexposed battery

As described by Stamm et al (2017), this zinc oxide accumulation caused by the reduction-oxidation reaction occurring within the battery attributes to zinc passivation and dendritic formation, the major failure mechanism of zinc air batteries [2, 8, 15, 16]. Since this value is vastly different between the battery that was exposed to air and the one encased during the experiment duration, it is highly supportive of the failure mechanisms identified by previous research.

After the exposed and unexposed batteries were analyzed, the difference between the exposed battery with respect to time was of great interest. The changes in both morphology and chemical composition lend to the explanations of failure mechanisms that are of the highest interest in the research of zinc-air batteries. When comparing the micrographs, the differences are evident between each day of the exposed battery sample. An important difference that is easily notable and observed is the growth from the smoother sections of the exposed battery from day 4 to day 7. These structures are presented in Figure 7 and 10 and reintroduced in Figure 25. In these figures, there are branching structures that appeared. This structure should be deemed as significant because of the similar findings in Riede et al., Banik et al., and Wang et al. [8, 11, 12]. All of these studies indicated that dendritic growth that mimics the structure found in the above SEM images, inhibited the life span and function of zinc air batteries. The mechanism that these structures work is through the short circuits they create at the anode by the accumulation of zinc oxide. Since the average lifespan of these batteries is only 3 to 7 days, the appearance of these branches at day 4 and disappearance after day 7, follows and agrees with the degradation mechanism by dendric formation that would occur at these times in a functioning battery cell. This is significant in showing that actual structures that branch and form the circuity issue with in the batteries. If this relationship can be quantified, further measures can be taken to prevent this structure formation in battery cells.

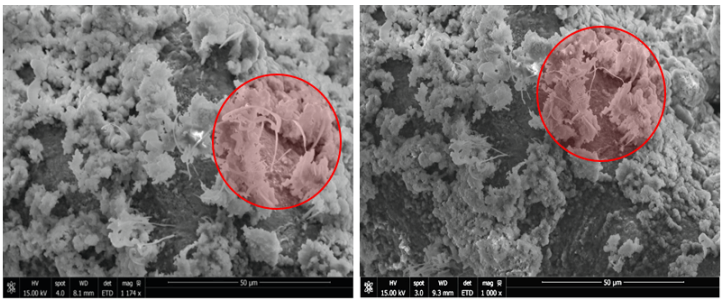

Figure 25 (A) Day 4 SEM photo of exposed battery presenting dendritic formation indicated in red at 1174x magnification; (B) Day 7 SEM photo of exposed battery presenting dendritic formation indicated in red at 1000x magnification.

Figure 14 to 16 show the differences between the intervals tested with exposure to oxygen. A comparison between the images from the first and second day shows clear evidence of particle break down represented by a change in surface smoothness. After seven days of exposure, there was a clear difference in smoothness of the surface of the particle. The interactive 3-D plots show that the depth of the particles decreases with exposure. The units going from micrometers to millimeters in day one to day seven represents this change. The magnification of the unexposed particle is comparable to that of days one and two. After the initial two days, the image magnification was increased to better analyze the particles. There were also chemical differences in these batteries during the study.

On days 2, 4, and 7, EDS data was collected for carbon, potassium, oxygen, and zinc. This data is displayed in Table 2. Although there were changes in all elemental present, the primary concern is oxygen. The manifestation of oxygen within the battery agrees with the prediction that zinc will undergo reduction-oxidation reactions when exposed to the atmosphere. As previously mentioned, the accumulation of zinc-oxide, the product of zinc oxidation, produces precipitation on the anode and dendritic growth. Both of these structures increase the frequency of failure in zinc air batteries, which is supported by Yang et al (2003), Wang et al (2018), and Fu et al (2017) [17–19]. The oxygen data was taken and used to create a graph in Figure 26 that represents the change in oxygen over time, which correlates to the rate of zinc oxidation within the battery cell. Using this data set, it can be observed that there is a linear relationship between days 2 and 4, and then a leveling of oxygenation after day 4. According to battery standards from Energizer, battery lives for a D13 battery, as used in this study, are between 3 and 5 days [20]. Since the data indicates maximum oxidation after 4 days, this coincides with the manufacturer's suggested life span when the battery is implemented in a hearing aid device. Because a linear relationship is observed, a mathematical relationship can be established that will predict the oxygen composition of the zinc air battery when left in room temperature environments from day 1 to 4 days. The equation can also be used to predict the rate at which zinc is oxidized. This mathematical definition for oxidation is presented in Equation (5).

Linear relationship of oxygen percentage composition verses days exposed to atmosphere:

$$y = 4.595x + 10.16 \tag{5}$$

Table 2 Percentages of carbon, oxygen, potassium, and zinc present in days 2, 4, 7 of the exposed battery.

Day	Element			
	Carbon	Oxygen	Potassium	Zinc
2	12.145	19.098	47.510	20.420
4	28.370	28.540	30.480	11.620
7	13.200	27.725	37.775	20.950

The importance of this equation in this study and others relates to the passivation and dendritic presence in used batteries that lead to short circuiting and ultimately battery failure. Equation 3 links the days exposed to the amount of oxygen in the battery compounds, which is further associated to the rate of passivation and dendritic formation.

The second experiment was incorporating the maximum oxidation at day 4. With maximum oxidation occurring after 4 days, exposure to oxygen was another area to experiment. With the time the anode was exposed to variable oxygen growth, the results confirm what is stated before, the unexposed battery being exposed to a small amount of oxygen and still having some

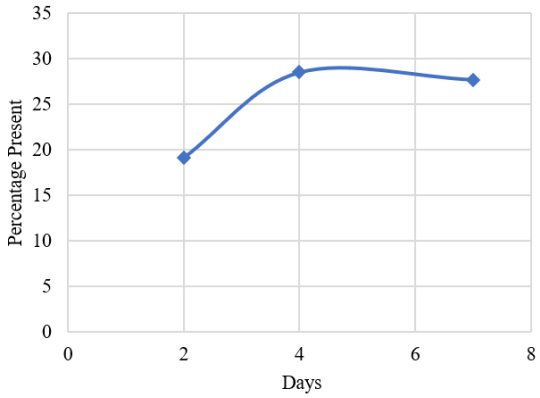

Figure 26 Graphical representation of data presented in Table 2 of only oxygen composition changes over the seven-day exposure period

oxidation occur. It is shown through Figure 17 to 22 the amount of oxidation increasing when the battery is exposed for a time period and then unexposed for 4 days. The images are shown at 300x magnification, on the left, and then 3000x, on the right. The oxidation increases with more exposure time, which is expected, but with a small exposure time the oxidation is still significant. At an exposure time for thirty minutes and two hours, the 3000x magnification images are similar in oxidation. This confirms that exposure to oxygen for a small period of time affects the approximate lifetime of the battery.

The SEM images also showed that the oxidation was not uniform throughout the battery, as a result of large, unevenly distributed areas of electrolyte.

6 Conclusion

Using the data gathered from this study, it can be determined that dendritic formation and passivation of zinc in zinc-air batteries due to oxidation compete and result in a short lifespan for the battery. Not only can this conclusion be made but also supported with a mathematical model that predicts the rate of oxidation. The 3-D interactive plots show the difference in depth of the particles with the difference in exposure through the 7 days compared to the unexposed battery. This is expected due to the battery outputting voltage from the chemical reaction between the zinc and oxygen.

Further research should be completed to connect the passivation and dendritic models proposed by prior literature. If the array of equations can confirm one another, a detailed understanding of the rate at which the chemical reaction occurs in the zinc-air batteries can be learned. Then, by altering the variables and observing the changes to the behavior of oxidation, adjustments can be made to extend the overall life span of these batteries. The voltage output in relation to the oxidation is another area that could be researched. This research could potentially change the design of zinc-air batteries, which would then prolong the lifespan.

Acknowledgements

The research was inspired by Mrs. Tandra Chatterjee as a part of 2 honors research project in Biomedical Engineering. United States Air Force Research Lab for the assistance with all battery experiments and SEM imaging.

References

[1] Minakshi M and Ionescu M. Anodic behavior of zinc in Zn-MnO2 battery using ERDA technique. International Journal of Hydrogen Energy, 2010, **35**(14): 7618-7622. https://doi.org/10.1016/j.ijhydene.2010.04.143

[2] Bockelmann M, Reining L, Kunz U, *et al*. Electrochemical characterization and mathematical modeling of zinc passivation in alkaline solutions: A review. Electrochimica Acta, 2017, **237**: 276-298. https://doi.org/10.1016/j.electacta.2017.03.143

[3] Liu MB, Cook GM and Yao NP. Passivation of Zinc Anodes in KOH Electrolytes. Journal of the Electrochemical Society, 1982, 128: 1663-1668. https://doi.org/10.1149/1.2124104

[4] Mainar AR, Iruin E, Colmenares LC, *et al*. An overview of progress in electrolytes for secondary zinc-air batteries and other storage systems based on zinc. Journal of Energy Storage, 2018, **15**: 304-328.
https://doi.org/10.1016/j.est.2017.12.004

[5] Schmid M and Willert-Porada M. Electrochemical behavior of zinc particles with silica based coatings as anode material for zinc air batteries with improved discharge capacity. Journal of Power Sources, 2017, **351**: 115-122.
https://doi.org/10.1016/j.jpowsour.2017.03.096

[6] Puapattanakul A, Therdthianwong S, Therdthianwong A, *et al*. Improvement of Zinc-Air Fuel Cell Performance by Gelled KOH. Energy Procedia, 2013, **34**: 173-180.
https://doi.org/10.1016/j.egypro.2013.06.745

[7] Kim H, Kim E, Kim S, *et al*. Influence of ZnO precipitation on the cycling stability of rechargeable Zn–air batteries. Journal of Applied Electrochemistry, 2015, **45**(4): 335-342.
https://doi.org/10.1007/S10800-015-0793-4

[8] Wang K, Pei P, Ma Z, *et al*. Morphology control of zinc regeneration for zinc–air fuel cell and battery. Journal of Power Sources, 2014, **271**: 65-75.
https://doi.org/10.1016/j.jpowsour.2014.07.182

[9] Toussaint G, Stevens P, Akrour L, *et al*. Development of a Rechargeable Zinc-Air Battery. The Electrochemical Society, 2010, **28**(32): 25-34.
https://doi.org/10.1149/1.3507924

[10] Chamoun M, Hertzberg BJ, Gupta T, *et al*. Hyper-dendritic nanoporous zinc foam anodes. Npg Asia Materials, 2015, **7**(4): e178.
https://doi.org/10.1038/am.2015.32

[11] Riede J, Turek T and Kunz U. Critical zinc ion concentration on the electrode surface determines dendritic zinc growth during charging a zinc air battery. Electrochimica Acta, 2018, **269**: 217-224.
https://doi.org/10.1016/j.electacta.2018.02.110

[12] Banik SJ and Akolkar R. Suppressing Dendrite Growth during Zinc Electrodeposition by PEG-200 Additive. Journal of The Electrochemical Society, 2013, **160**(11): 519-523.
https://doi.org/10.1149/2.040311jes

[13] Kim H and Shin H. SnO additive for dendritic growth suppression of electrolytic zinc. Journal of Alloys and Compounds, 2015, **645**: 7-10.
https://doi.org/10.1016/J.JALLCOM.2015.04.208

[14] Wang J, Zhang L, Zhang C, *et al*. Effects of bismuth ion and tetrabutylammonium bromide on the dendritic growth of zinc in alkaline zincate solutions. Journal of Power Sources, 2001, **102**(1-2): 139-143.
https://doi.org/10.1016/s0378-7753(01)00789-3

[15] Stamm J, Varzi A, Latz A, *et al*. Modeling nucleation and growth of zinc oxide during discharge of primary zinc-air batteries. Journal of Power Sources, 2017, **360**: 136-149.
https://doi.org/10.1016/J.JPOWSOUR.2017.05.073

[16] Minakshi M and Ionescu M. Anodic behavior of zinc in Zn-MnO2 battery using ERDA technique. International Journal of Hydrogen Energy, 2010, **35**(14): 7618-7622.
https://doi.org/10.1016/J.IJHYDENE.2010.04.143

[17] Yang H, Cao Y, Ai X, *et al*. Improved discharge capacity and suppressed surface passivation of zinc anode in dilute alkaline solution using surfactant additives. Journal of Power Sources, 2004, **128**(1): 97-101.
https://doi.org/10.1016/J.JPOWSOUR.2003.09.050

[18] Wang K, Pei P, Wang Y, *et al*. Advanced rechargeable zinc-air battery with parameter optimization. Applied Energy, 2018, **225**: 848-856.
https://doi.org/10.1016/J.APENERGY.2018.05.071

[19] Fu J, Cano ZP, Park MG, *et al*. Electrically Rechargeable Zinc– Air Batteries: Progress, Challenges, and Perspectives. Advanced Materials, 2017, **29**(7): 1-34.
https://doi.org/10.1002/ADMA.201604685

[20] Application Manual: Zinc Air [PDF]. (n.d.) St. Louis, MO: Energizer.